

## Grafting of Dissolved Pulp from Date Palm Byproducts for Use in Industrial Water Purification

Maha S. Elsayed<sup>1\*</sup>, Alaa M.M. EL-Torky<sup>2</sup>, Gadalla, E.G.<sup>1</sup>

<sup>1</sup>The Central Laboratory for Date Palm Researches and Development, Agricultural Research Center, Giza, 12619, Egypt.

<sup>2</sup>Department of chemistry, Faculty of Science, Zagazig University, Zagazig, Egypt.

### Abstract

Date palm (*Phoenix dactylifera* L.) is considered as an important crop in the Arabian Gulf. Lot of date palm leaves and rachis were collected annually and considered waste that causes problem for the environment. In this work, the cellulose fiber was isolated from two by-products of the date palm tree, rachis, and leaflets by acid hydrolysis and bleaching treatments. The isolated cellulose fiber was modified by grafting with acrylamide to convert into composite polymer to use in the purification of waste water. There are numerous advantages to using isolated cellulose fiber and its composite polymer. This fiber is widely used in modern industries and has replaced conventional materials due to their high specific strength, light weight, low cost, recyclability, biodegradability, and long durability. All prepared samples were characterized by Fourier transform infrared, X-ray diffraction, the energy dispersive X-ray and scanning electron microscopy. The results obtained indicate that the percent of cellulose was increased and the percent of lignin and hemicellulose was decreased after the isolation and bleaching processes and the cellulose fiber obtained from date palm by-products characterized by high crystallinity. Grafted samples copolymers were used in removal of methyl orange from waste water to study the role of cellulose grafted samples in purification of it as an application in our study. The maximum adsorption of MO occurs at pH 3.0 after 15 h, and the maximum adsorption capacity calculated from Langmuir is 48.12 mg/g. Date palm fibers considering as a promising alternative substitute to synthetic fibers in polymer composite industry.

**Keywords:** Grafted cellulose, Date palm tree, Removal of MO

\*Corresponding author: [maha.sobhy@arc.sci.eg](mailto:maha.sobhy@arc.sci.eg) or [mahasobhy1000@yahoo.com](mailto:mahasobhy1000@yahoo.com)

### Introduction

Date palm tree has an economic importance especially in the Middle East and North Africa (Ahmed *et al.*, 1995). Its cultivation and population is on increase in the Gulf region. Now days, there is an increased interest towards the using agricultural by-products from agro-industries (Alvarez *et al.*, 2011). Date palm pits and leaves are waste materials that used in producing natural fibers and activated carbon (Mahdavi *et al.*, 2010). These trees generate tons of leaves, rachis and trunk as wastes; a lot of them are converted to compost and using for traditional art and craft or burned causing contamination to environment. Date palm fiber can use as alternative to synthetic fibers in polymer composite industries (MaCC *et al.*, 1998). Natural fiber is used to improve efficiency of many mechanisms, and has great attraction to use as bio-fillers due to low cost and non-carcinogenic compared to synthetic fibers (Jawaid and Khalil, 2011). Few studies deal with fibers isolated from date palm byproducts some of them are succeed in using these fibers for reinforcing composites (Agoudjil *etal.*, 2011; Al-Sulaiman, 2003; Kaddami *et al.*, 2006; Sbiai *et al.*, 2010), and for water treatment as eco-friendly flocculants or filters (Riahi *et al.*, 2009; Khiari *etal.*, 2010). The isolation of cellulose and producing different types of paper pulp has less attention. Acid-alkali consider as effective method to isolate cellulose from the material that has lignocellulose structure (Ching and

Ng, 2014; Sheltami *et al.*, 2012). Cellulose is the most abundant natural polymer on earth (Zhang and Lynd., 2006; O'Sullivan., 1997). Cellulose can be used to produce high-value chemicals and polymer composites (Kumar *et al.*, 2017; Yang *et al.*, 2016; Brinchi *et al.*, 2013; Reyes-Luyanda *et al.*, 2012). It is the main constituent of a plant cell wall, Cellulose is linear homopolysaccharide composed of repeating  $\beta$ -(1 $\rightarrow$ 4) linkage between D-glucose units, its general formula is  $(C_6H_{10}O_5)_n$ , where n is the number of repeated monomeric  $\beta$ -d-glucopyranose units and different with the source of the cellulose (Kumar *et al.*, 2017). Cellulosic fibres are form in nature in two shape; the first type of fibres are that found in fibre form and last type that embedded in a natural matrix inside the plant. the last type needs several steeps as delignification and/ or extraction processes. These processes could be chemical, biological, mechanical or a combination of them (Elseify *et al.*, 2020) Methyl orange (MO) is an aromatic anionic dye, which causes problem at low concentration (Hassanzadeh-Tabrizi, *et al.*, 2016). Long exposure to MO causes problem in inhalation, heaving and looseness of the bowels, so it is necessary to remove MO from wastewater before releasing into nature. There are numerous ways used to remove dyes from industrial water as biodegradation (Sun *et al.*, 2017), Fenton oxidation (Gonzalez-Bahamon *et al.*, 2011), catalysis (Lin *et al.*, 2015), photocatalysis (Bhattacharya *et al.*, 2019), adsorption (Li *et al.*, 2018). Adsorption method is considering the most favorable method to remove dyes (Youssef *et al.*, 2019), it characterized by low costs and low energy use (Liu *et al.*, 2015). Grafting of cellulose is one of the most important means to improve the natural and chemical properties of cellulose and increase the ability of cellulose to absorbed chemical pollutant from drinking water and industrial water. Grafting copolymer was prepared from isolated cellulose and acrylamide in presences of persulphate as initiator (EL-Torky, *et al* 2017). The produced copolymer was used to eradicate MO from industrial water by adsorption. The effect of concentration, pH and time were discussed. Chemical characterization of isolated cellulose and produced copolymer carried out by Nicolet Model FTIR. Texture characterization done by X-ray diffraction (XRD) using a (Bruker AXS D8 Advance), Scanning electron microscope (Quanta 250 FEG) and Energy Dispersive X-ray. The degree of absorption of methyl orange from solution illustrated and determined using Langmuir and frendlich equations. The purpose of this paper is isolation of cellulose fiber from rachis and leaflet of date palm tree and making grafting process to the isolated cellulose after that studying the role of isolated cellulose samples in the purification of industrial water from MO.

## Materials and methods

### 2.1. Raw materials

Two by-products from *Phoenix dactylifera* L. were used in this study; the palm by-product samples was collected from Taj El-Ezz research station, Dakahlia governorate. The samples were washed with deionized water to remove dirt and dried (in shaded area), then cut, milled and collected through a 5 mm diameter mesh before chemical analysis. Acrylamide, potassium per sulphate PPS, sodium hydroxide, methyl orange and all the solvents were obtained from Sigma Aldrich. Fig. 1 shows morphology of by- product date palm tree which used in this study.



**Fig (1):** Morphology of by- product date palm tree (a) Leaflet (b) Rachis.

## 2.2. Get cellulose from date palm tree (rachis and leaflet)

The isolation of cellulose from by-product of date palm tree needs pretreatment to remove resins waxes and solubilizes the lignin and hemicellulose, also to increase the cellulose quantity in the biomass. Cellulose dissolving pulp obtained in this study from rachis and leaflet of date palm tree by three steps to remove the major part of lignin and hemicellulose. (a) Prehydrolysis step by using rachis and leaflet of date palm tree and  $H_2SO_4$ , (b) pulping step by soda ( $NaOH$  /1N), then wash with distilled water and treated with diluted HCL, mechanical stirrer to break down the cell walls, wash again, then filtered to obtain the cellulose fibers (Boldizar *et al.*, 1987). The final step; the delignification of residual lignin was carried out by hydrogen peroxide/ sodium hydroxide bleaching process ( $H_2O_2/NaOH$ ). After bleaching, pulp obtained was washed with deionized water until pH 7, and then dried in air.

## 2.3. Grafting of acrylamide onto isolated cellulose

Graft copolymerization of acrylamide onto isolated cellulose was carried out with  $K_2S_2O_8$  (PPS) as an initiator under vacuum. In a nicked 250 ml flask  $K_2S_2O_8$  is added to 2 g of isolated cellulose and 30 ml distilled water then put the solution in water bath at 80 °C for 15 min, then solution of acrylamide was added in flask and shaking for 3 h. The products were precipitated and dry it to obtain constant weight. The cellulose grafted samples immersed in distilled water for 24 hr to remove homopolymer, filter then let the sample dry in air (Mostafa *et al.*, 2007).

## 3. Characterization

### 3.1. Chemical composition of date palm by products

Chemical constituents of rachis, leaflet and isolated cellulose were measured according to ASTM standards.  $\alpha$ -cellulose (ASTM D 1103-55T), hemicelluloses (ASTM D1104-56), lignin (ASTM D1106-56). Also ash content of all samples was discussed.

### 3.2. Fourier Transform Infra-Red Spectroscopy (FT-IR)

FT-IR were done and collected in the absorbance mode from 4000 to 400  $cm^{-1}$  using (10 Nicolet Model FTIR- made in (USA)). IR spectra of isolated cellulose and grafted cellulose – acrylamide copolymer were recorded.

### 3.3. Scanning Electron Microscopy (SEM)

Scanning Electron Microscope (Quanta 250 FEG) running at a high voltage of 15 kV was used to study surface morphology. The samples were covered with gold by a gold sputtering for perfect visibility, then placed on the sample holder to examination (Rosas *et al.*, 2009 and Somasundaram *et al.*, 2013).

### 3.4. X-ray Diffraction Technique (XRD)

X-ray diffraction done by (Bruker AXS D8 Advance) diffractometer at a scanning rate of 5°C per min with Cu K  $\alpha$  radiation source ( $\lambda = 1.54060 \text{ \AA}$ ) and operating at 45 kV and 30 mA. Samples were placed in a 2.5 mm deep cell and the XRD patterns were obtained at  $2\theta = 4^\circ - 80^\circ$ . The crystalline structure of the all samples was examined. The crystallinity index was estimated by means of the peak height method and applying of equation (1) of (Segal *et al.*, 1959).

$$CI = \frac{I_{002} - I_{am}}{I_{002}} * 100 \quad (1)$$

Where  $I_{002}$  is the peak intensity at  $2\theta = 16^\circ$  and  $I_{am}$  is the peak intensity at  $2\theta = 22^\circ$ .

### 3.5. The energy dispersive X-ray (EDX)

EDX analyses of the samples were carried out using Oxford Link Isis (UK) instrument. In addition, the elemental analyses for selected samples were studied.

### 3.6 Adsorption Studies of Methyl orange

Set adsorption equilibrium experiments were conducted for the adsorption of MO on grafting samples by adding 0.1g of samples to 50 mL of MO with numerous concentrations (50-400 mg/L) at constant vibrating speed (150 rpm). After that residual MO concentration was calculated at a wavelength of 464 nm by spectrophotometer (UV-1700 Shimadzu, Japan). Adsorbed amount  $q_e$  (mg/g) was calculated:

$$q_e = \frac{(C_0 - C_e)V}{M} \quad (2)$$

Where  $C_0$  and  $C_e$  is the initial and equilibrium liquid phase concentration of MO (mg/L), respectively.  $V$  is the volume of solution (L), and  $M$  is the amount of adsorbent used (g).

The impact of pH on MO adsorption of MO was discussed; the experiments were carried out at pH varied from 2 to 11 at constant initial concentration of 200 mg/L. The pH of solution was adjusted by 0.1 M NaOH or 0.1 M HCl. The concentration of MO was done by double beam UV-visible spectrophotometer.

Effect of time was done by adding 0.1 g of adsorbent with 50 mL of MO solution at concentration 200 mg/L. The concentration of adsorbate after recorded time is calculated; the adsorption capacity at time  $t$ ,  $q_t$  (mg/g) was determined as follows:

$$q_t = \frac{(C_0 - C_t)V}{M} \quad (3)$$

## Results and discussion

### 4.1. Chemical analysis for raw material

The isolation of cellulose from by-product of date palm tree needs pretreatment of the biomass to eliminate resins, waxes, lignin and hemicellulose. Fig. 2 shows the physical appearance of the extracted cellulose, which has dark brown color before bleaching. Color of samples was changed after bleaching and acidification, the bleaching process remove residual lignin that remained in samples after pulping stage

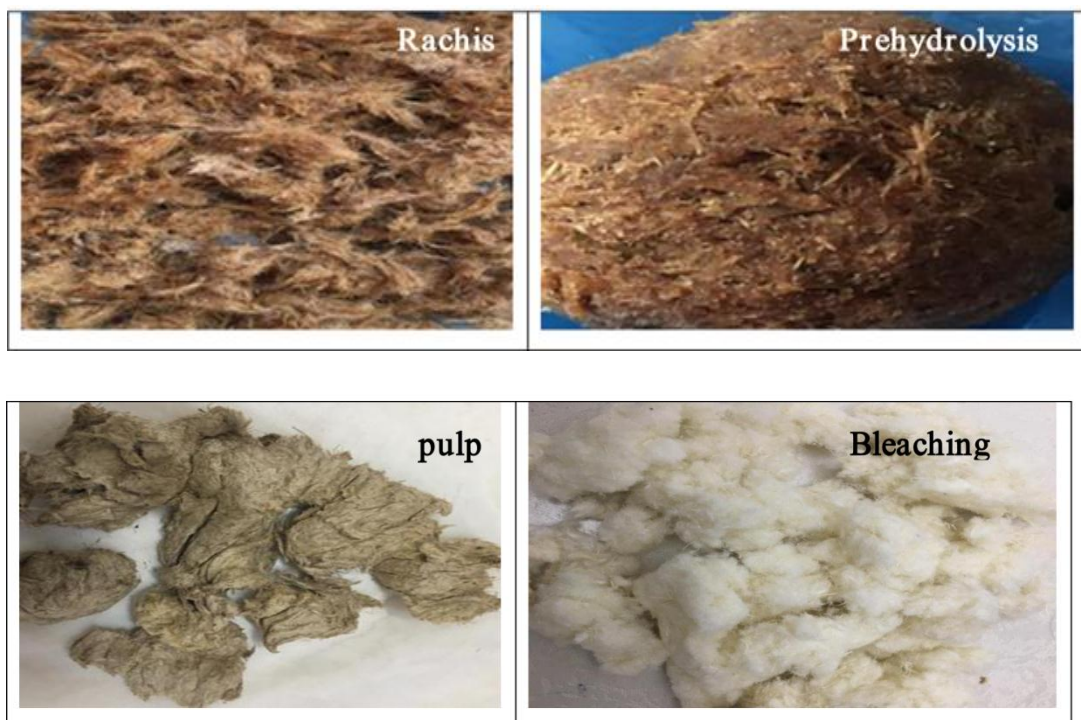


**Fig (2):** Physical appearance of the stage to isolate cellulose

Chemical composition of the rachis, leaflet and bleached sample was carried according to standard method and the data are listed in Table 1 and showing that: (i) The bleached sample give high yield of cellulose which increase from 43.08 to 67.37 % in the sample of rachis and also increase in case of leaflet from 34.55 to 68.50% this increase in the percent of cellulose due to alkali treatment during chemical extraction. (ii) High yields of cellulose represented that date palm by product consider as a good source of cellulose and draw attention to green economic growth due to its cost. (iii) Ash percent in case of bleaching samples is low compared with the other samples due to sodium hydroxide dissolved apart of ash.

**Table (1)** Chemical composition of raw material and bleached samples

Sample	Hemicelluloses %	Cellulose %	Lignin %	Ash %
Rachis	23.92	43.08	15.14	5.23
Isolated cellulose from rachis	15.77	67.37	5.00	0.31
Leaflet	27.52	34.55	19.28	6.00
Isolated cellulose from leaflet	14.89	68.50	5.12	0.38



## 4.2. FTIR spectroscopy analysis

FTIR spectroscopy is a simple technique that used in cellulose research that giving information about chemical changes which appears during chemical treatments (Ristolainen *et al.*, 2002). Fig. 3 (a, b) compares the FTIR spectra of isolated cellulose fibers from rachis, leaf let and grafted cellulose – acrylamide, from the figure we found that in cases of isolated cellulose samples the disappearance of the lignin-associated absorbance band at 1600 and 1510  $\text{cm}^{-1}$ . There is broadband appear at 3400 this band related to the adsorbed water, at 2919  $\text{cm}^{-1}$  there is a band for C-H stretches and  $\text{CH}_2$  symmetric bending. Also there is a band at 1029  $\text{cm}^{-1}$ , due to C-O band stretching, while in case of grafted cellulose-acrylamide samples, there is a new band at 1690  $\text{cm}^{-1}$  in spectrum which is attributed to carbonyl group C=O of amide.

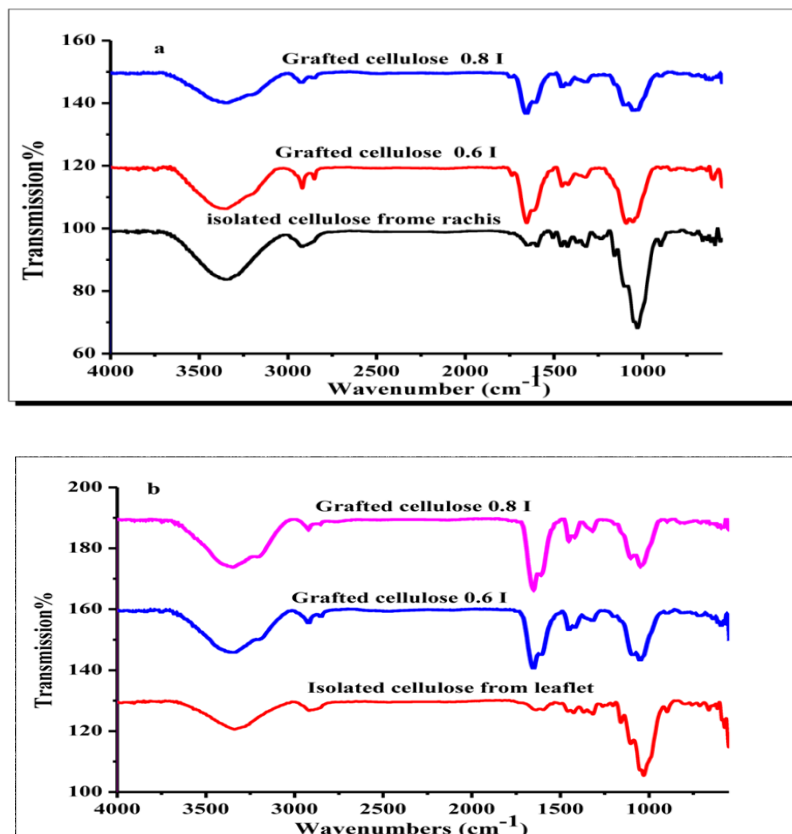


**Fig (3):** FT-IR spectra of (a) isolated cellulose from rachis and grafting cellulose/acrylamide; (b) isolated cellulose from leaflet and grafting cellulose/acrylamide.

## 4.3. Scanning electron microscopy (SEM)

SEM is used to detect the differences in surface morphologies among all the samples at magnitude 200. Fig. 4 (a, b, c) represented images of the celluloses isolated from rachis, grafting cellulose /acrylamide samples with different concentration of initiator (pps). It is clear that the isolated cellulose produced from rachis has skeletal rod-like macrofibril structures with an identifiable form and well-defined cylindrical rod-like detected in the rachis, these images show removal of hemicelluloses and lignin after bleaching and the fiber where dispersed into individual fibers. SEM images of cellulose samples extracted from leaflet, grafting cellulose/ acrylamide with different concentration of initiator are shown in Fig. 4 (d, e, f), showed that chemical treated fibers showing growth in tensile strength and celluloses fiber from leaflet showing high porous with an appreciable diameter which able to remove MO dye. In addition, the weak outer layer was isolated during chemical treatment leading to

strong connection with the matrix which found in the polymer composites. The results showing improvement in morphology.

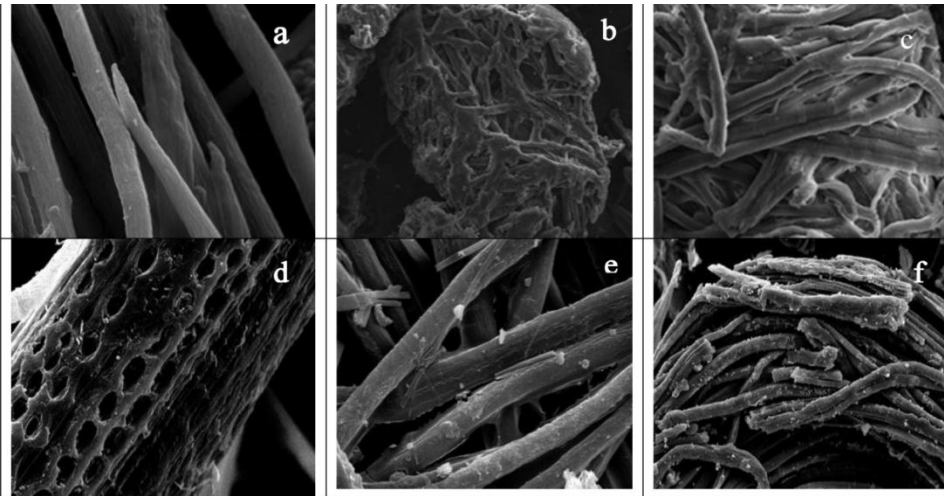


**Fig (4):** SEM images of (a) isolated cellulose from rachis, (b) grafting cellulose/acrylamide 0.6 initiator (c) grafting cellulose/acrylamide 0.8 initiator (d) isolated cellulose from leaflet (e) grafting cellulose /acrylamide 0.6 initiator and (f) grafting cellulose/acrylamide 0.8 initiator.

#### 4.4. X-ray Diffraction analysis

XRD spectra of isolated cellulose fibers from rachis, leaflet and its grafted cellulose-acrylamide was shown in. Fig 5 (a ,b) . There is a major crystalline peak for isolated cellulose appear at  $2\theta = 16$  and  $22$ , which characterize the cellulose crystallographic plane and related to hemicelluloses and alpha-cellulose. This is assumed typical cellulose-I structure. Same results were obtained by (Rosa *et al.*, 2012) for chlorine-free cellulose isolated from rice and whisker. Crystalline arrangements in the cellulose occurs owing to formation of inter and intramolecular H-bonding by the hydroxyl groups (Chirayil *et al.*, 2014). The H-bonding restricts the free movement of the cellulosic chains and chains align close together in an orderly manner which tends to have the crystallinity. Also, there is additional crystal lattice at  $30^\circ$  and  $48^\circ$  the same results appear in the XRD of bacterial cellulose/silver nano composites (Zhijiang *et al.*, 2011). The higher crystallinity raises rigidity, stiffness and improvement mechanical properties. The crystal lattice and high crystallinity of the isolated celluloses from rachis and leaflet promise to enable the development of nanocomposites with improved mechanical properties.

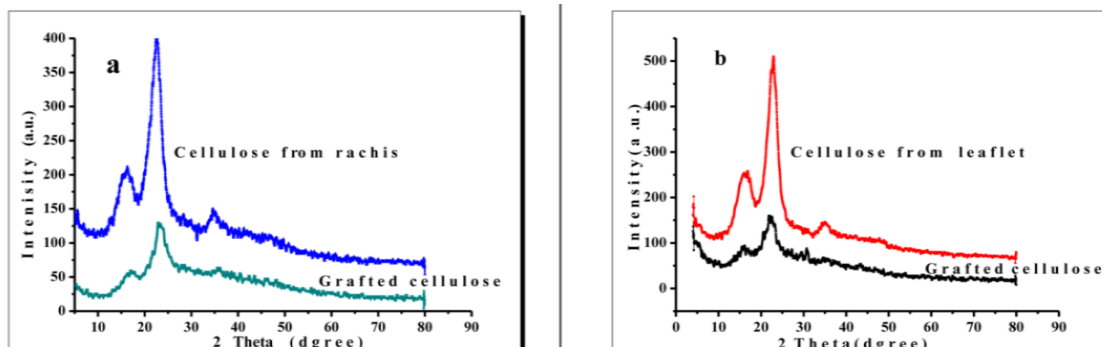


**Fig (5):** (a) X-ray of isolated cellulose from rachis and grafting cellulose/acrylamide; (b) isolated cellulose from leaflet and grafting cellulose/acrylamide.

#### 4.5. The energy dispersive X-ray (EDX)

Energy dispersive x-ray was used for determining elemental analysis of isolated cellulose from rachis, grafting cellulose/acrylamide, isolated celluloses from leaflet and grafting cellulose/acrylamide respectively. From Fig. 6 (a, c) we found that there is a peak for carbon and oxygen in case of isolated cellulose from rachis and leaflet. On the other hand, Fig 6. (b, d) represented the appearance another peak which corresponding to potassium as we used potassium per sulphate as initiator. Isolated cellulose from rachis and leaflet contain carbon (54.2, 51.4 wt. %) and oxygen (45.71, 48.59%). While in case of grafting cellulose from rachis and leaflet contain carbon (50.91, 49.03 wt %) oxygen (47.71, 48.88%) and potassium (1.99, 2.10) due to using of potassium per sulphate as initiator in grafting process.

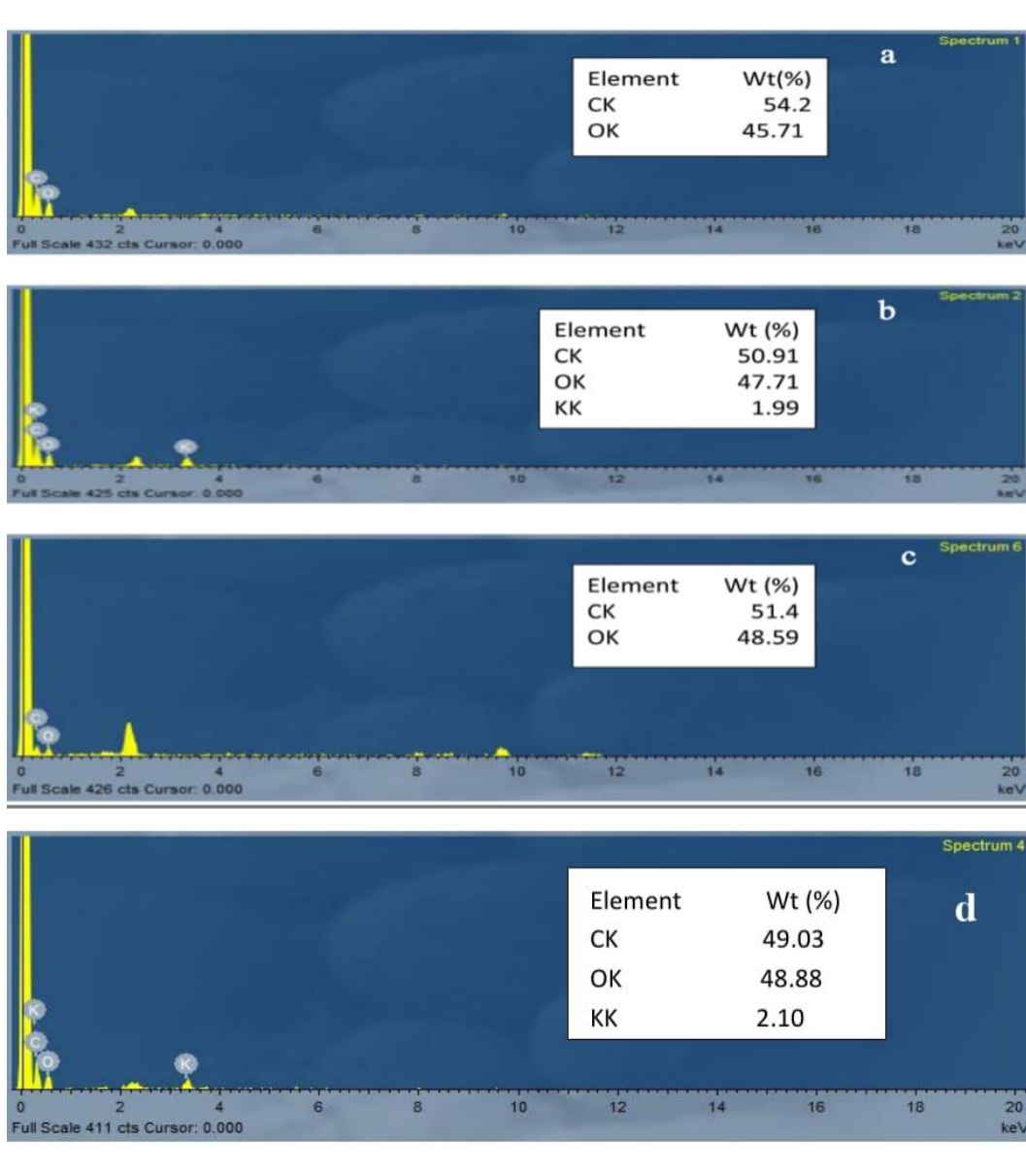


**Fig (6):** EDX spectrum of (a) isolated cellulose from rachis, (b) grafting cellulose/acrylamide 0.6 initiator, (c) isolated cellulose from leaflet, (d) grafting cellulose /acrylamide 0.6 initiator.



## 4.6. Adsorption of Methyl Orange

### 4.6.1. Effect of pH

The pH value is considered as important factor for adsorption performance; it is also effect on physical and chemical properties of the adsorbent surface (Liu *et al.*, 2016).The experiment was studied at pH (3, 5, 7, 9 and 11) to reach the impact pH of MO removal using grafting cellulose/ acrylamide isolated from rachis and leaflet. Fig.7 showed the adsorption of MO reached the maximum value at pH 3.0, after that decreasing trend at pH 11.0 appears. This varying in pH value leads to change in the charge property of adsorbent surface and the species of adsorbate in solution. There is an electrostatic attraction between the adsorbent which has a positive charge in acidic liquid phase and draws negative molecules of MO as shown in Fig.8. Also, hydrogen particles made bridging ligands between the adsorbent and MO (Gupta *et al.*, 2013). When pH increases, the removal of MO decrease. This is owing to anionic dye solution competing with extra OH<sup>-</sup> (Mahmoodian *et al.*, 2015).

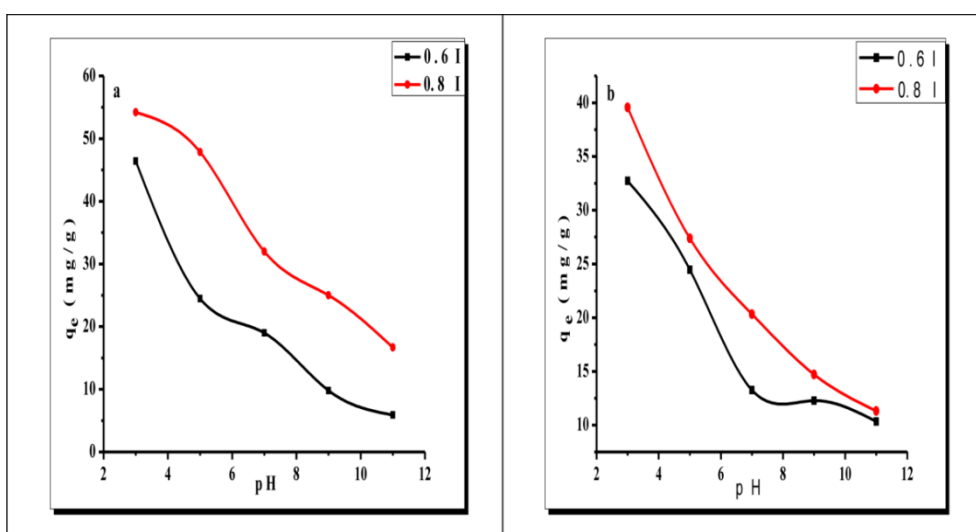


**Fig (7):** Effect of pH on adsorption of MO using grafting Cellulose/Acrylamide from (a) rachis and (b) leaflet as adsorbent

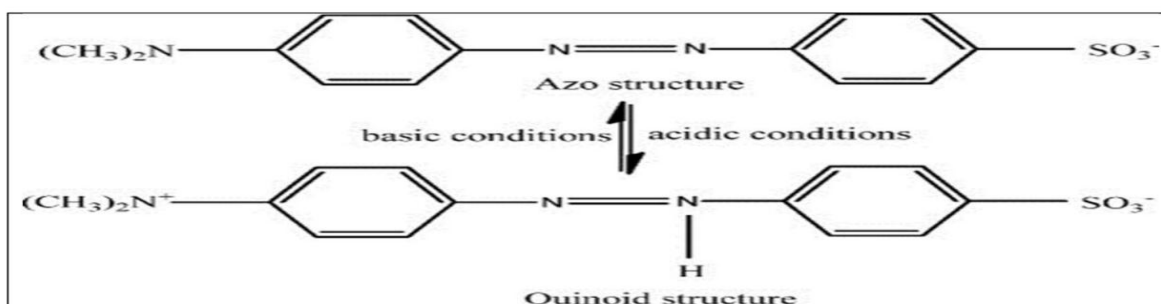


**Fig (8):** Chemical structure of methyl orange in acidic and basic condition

### 4.6.2 Effect of contact time and kinetic studies

It is vital to determine the adsorption rate and the time which needed to attain equilibrium. There are different models used to study kinetics of the solid-liquid adsorptionas, (Simonin, 2016) pseudo-first order kinetic model, (Li *et al.*, 2014) and the pseudo-second order kinetic model (Ho and Ofomaja,

2006) which applied to simulate the adsorption kinetics. Fig. 9 showed adsorption of methyl orange onto grafting cellulose/ acrylamide samples from rachis and leaflet. It clear that adsorption equilibrium reaches at 15 h and removal of MO on grafting samples was slightly improved in first of reaction due to there are a lot of vacant sites available which led to fast increase of adsorption in first period and the adsorption capacity gradually increases with time till reaching equilibrium at 15h. After this time there is no change as the reaction reach to balance so this time is sufficient to remove MO.

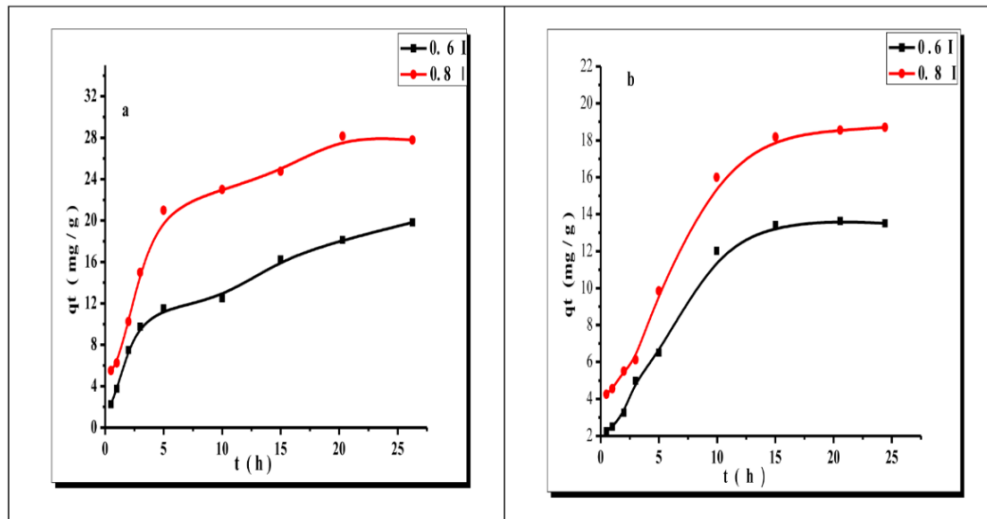


**Fig (9):** Kinetic adsorption curves of MO at 25 °C for cellulose/acrylamide samples from (a) rachis and (b) leaflet

The variant of dye adsorption versus time was determined according to both models of (pseudo-first order model and second) as clear in Eq. (3, 4) (He *et al.*, 2018). The linearized form of the PFO can be expressed as

$$\log(q_e - q_t) = \log q_e - \frac{K_1}{2.303} t \quad (4)$$

Where  $q_e$  is the equilibrium adsorbed amount (mg/g),  $q_t$  is the amount adsorbed in time  $t$  (mg/g),  $K_1$  is the pseudo-first-order rate constant (g/mg. min) and  $t$  is the time in minute. The linearized form of the PSO can be expressed as

$$\frac{t}{q_t} = \frac{1}{K_2 q_e} + \frac{1}{q_e^2} t \quad (5)$$

Where  $K_2$  is the pseudo second order rate constant (g/mg. min) (Fig. 10,11) illustrate use of linear form of PFO and PSO model for both grafting cellulose / acrylamide samples from rachis and leaflet respectively. Upon analysis of Table 2 one can concluded that the adsorption follow PSO kinetics model based on: (i) Correlation coefficient  $R^2$  in case of PSO is higher than  $R^2$  in case of PFO indicating that good applicability of PSO model. (ii) Calculated  $q_e$  (mg/ g) in case of PSO are closer to the value of  $q_m$  (mg/g) in case of Langmuir model.

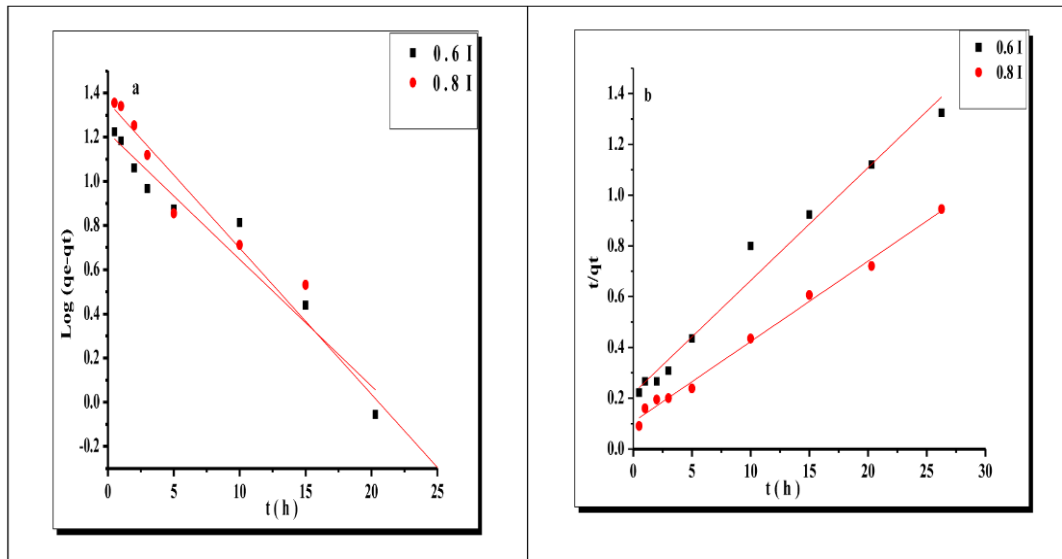


**Fig. (10):** (a) Pseudo–first order and (b) Pseudo–second order kinetic model for adsorption of MO onto investigated grafting cellulose/ acrylamide samples from rachis

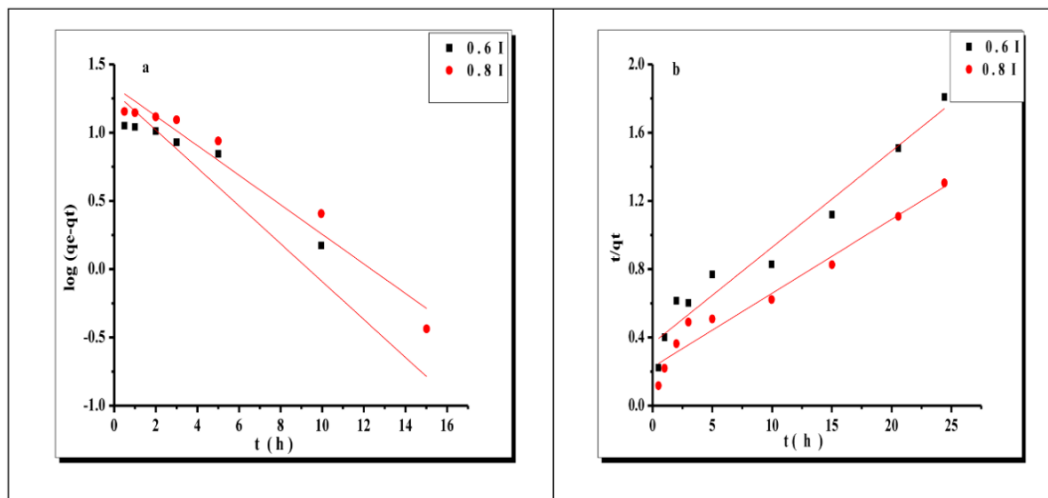


**Fig. (11):** Pseudo–first order and Pseudo–second order kinetic model for adsorption of MO onto investigated grafting cellulose/acrylamide samples from leaflet

**Table (2):** Kinetic model parameters (PFO and PSO) for adsorption of MO onto investigated grafting Cellulose/ acrylamide samples from rachis and leaflet

Sample	$q_m(\text{mg/g})$	PFO - kinetic model			PSO - kinetic model			
		$q_e (\text{mg/g})$	$K_1 (\text{h}^{-1})$	$R^2$	$q_e (\text{mg/g})$	$K_2 (\text{g/ mg h})$	$R^2$	
Rachis	0.6 I	8.403	16.622	0.1260	0.9456	22.52	$9.025 \cdot 10^{-3}$	0.97226
	0.8 I	19.23	22.855	0.1524	0.9688	31.565	$9.433 \cdot 10^{-3}$	0.9928
Leaflet	0.6 I	11.85	19.815	0.3178	0.92191	7.246	0.0523	0.95148
	0.8 I	48.123	21.777	0.2494	0.9368	42.37	$5.6211 \cdot 10^{-4}$	0.95601

### 4.6.3 Adsorption isotherms

It is vital factor to study mechanism of adsorption. The quantity of MO adsorbed,  $q_e$  (mg/g) is plotted versus the equilibrium concentration  $C_e$  (mg/L), as presented in Fig. 12 which indicated that adsorption capacity of MO by grafting copolymer of rachis and leaflet with acrylamide at adsorption equilibrium ( $q_e$ ) progressively increased with raising the initial MO concentration from 50 to 500 mg/L owing to as the initial concentration raised, the mass transfer driving force become higher, and this behavior will leads to higher adsorption of MO.

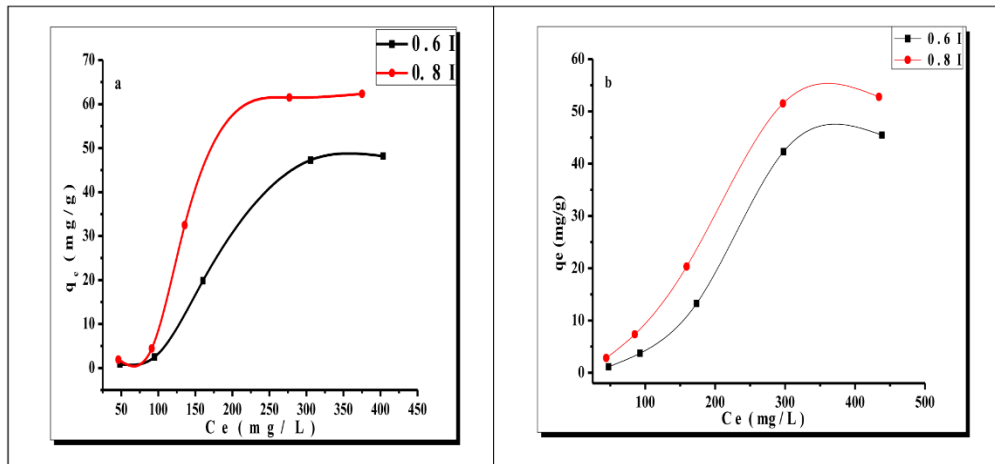


**Fig (12):** Adsorption isotherm of MO at 25 °C for grafting cellulose/acrylamide samples from (a) rachis and (b) leaflet

In this study, the isotherm of Langmuir and Freundlich were used to describe the distribution of MO on surface of grafting samples which isolated from rachis and leaflet. Langmuir supposed that only monolayer adsorption can take place on a homogeneous surface, (Brdar, *et al*, 2012), the Langmuir equation 6 is represented by (Langmuir, 1918).

$$\frac{C_e}{q_e} = \frac{1}{b q_m} + \frac{C_e}{q_e} \quad (6)$$

Where  $q_e$  is the amount adsorbed at equilibrium (mg/g),  $C_e$  is the equilibrium concentration of MO (mg/L),  $q_m$  represented the monolayer capacity (mg/g), and  $b$  is known as the Langmuir constant (L/mg) and it is related to the heat of adsorption. The plot of  $C_e/q_e$  versus  $C_e$  for grafting cellulose/acrylamide samples from rachis and leaflet give a straight line with slope =  $1/q_m$  and an intercept =  $1/bq_m$ , as shown in Fig. 13 (a) and Fig.14 (a) respectively and dimensionless separation factor ( $R_L$ ) as represented in Eq. (7)

$$R_L = \frac{1}{1 + b C_o} \quad (7)$$

Freundlich model is applied in case of hetero generous surface. The linear equation form is represented as:

$$\ln q_e = \ln K_f + \frac{1}{n} \ln C_e \quad (8)$$

Where  $K_f$  and  $n$  are freundlich constants which related to adsorption capacity and adsorption intensity, respectively. When  $n > 1$  this means that adsorbate is favorable but when  $n < 1$  this means adsorption process is chemical in nature, If  $n$  lies between 1 and 10, this means a favorable sorption process. The plot of  $\ln q_e$  versus  $\ln C_e$  gave straight line with slope  $1/n$  and intercept of  $\ln K_f$  as shown in Fig. 13 (b) and Fig.14 (b) for rachis and leaflet respectively. The examined data listed in Table 3 presenting that the correlation coefficient,  $R^2$  in case of freundlich model was in between 0.9272 and 0.9828 this means that the process of removal MO by grafting copolymer acrylamide

samples perhaps multi-layer adsorption. The  $n$  value of the Freundlich is a parameter that judges if the adsorption is spontaneous, the  $n$  values obtained from the Freundlich model is below 1 suggesting that the spontaneity of the adsorption (Zhang, *et al*, 2020).

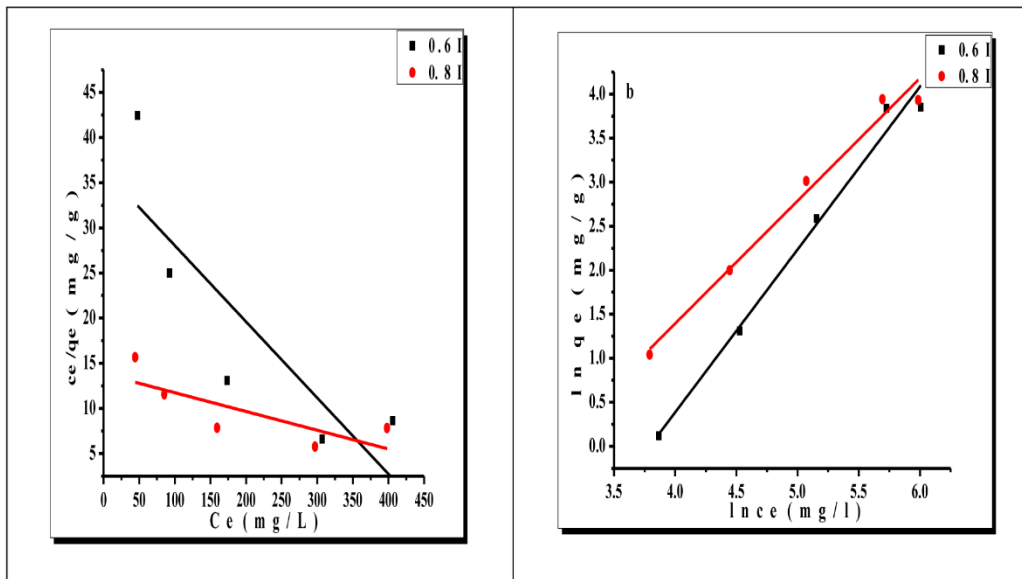


**Fig. (13):** (a) Linear plots of Langmuir and (b) Freundlich model for adsorption of MO onto investigated grafting cellulose/acrylamide samples from rachis

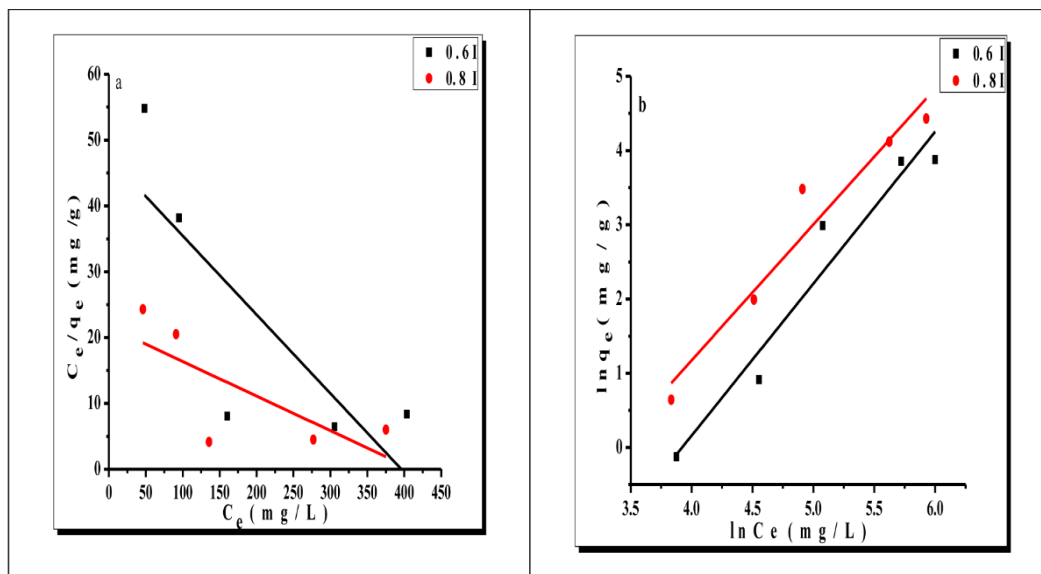


**Fig. (14):** (a) Linear plots of Langmuir and (b) Freundlich model for adsorption of methyl orange onto grafting cellulose/acrylamide samples from leaflet



**Table (3):** Langmuir and Freundlich constant for methyl orange at 25°C by the investigated grafting cellulose/acrylamide samples from rachis and leaflet

Sample		Langmuir				Freundlich		
		q <sub>max</sub> (mg/g)	b (L/mg)	R <sup>2</sup>	RL	K <sub>f</sub> (mg/g)	n	R <sup>2</sup>
Rachis	0.6 I	8.403	2.509*10 <sup>-3</sup>	0.529	0.443	2.142*10 <sup>-3</sup>	0.48841	0.92854
	0.8 I	19.23	2.403*10 <sup>-3</sup>	0.3990	0.499	3.253*10 <sup>-4</sup>	0.54650	0.92727
Leaflet	0.6 I	11.85	2.312*10 <sup>-3</sup>	0.6260	0.463	9.0461*10 <sup>-4</sup>	0.5409	0.98287
	0.8 I	48.123	1.50*10 <sup>-3</sup>	0.4867	0.571	0.01536	0.7181	0.97724

## Conclusion

The different experiments were done to discuss the influence of (contact time, pH and concentration) on adsorption of grafting dissolving pulp for MO dye. Chemical constituents of rachis, leaflet and isolated cellulose were measured, also percent of ash content of all samples were determined. Based on the present investigation, it could be assumed that grafting of dissolving pulp prepared from acrylamides and two byproducts from *Phoenix dactylifera* L. (rachis and leaflet each alone) using (PPS) as initiator can be used efficiently in removal of heavy MO dye from industrial water. The removal of MO dye was 200ppm, pH and contact time dependent, the maximum adsorption capacity at pH =3 and as the pH increases (pH > 3), the adsorption capacity decreases as a consequence and 15h was considered sufficient time for removal of MO. Also, Freundlich model coordinated with the isothermal experimental data quite well, and illustrated that the adsorption was a multilayer process and MO adsorption follows PSO model. Furthermore, based on the results of examining SEM, EDX, XRD combined with FTIR. Overall, the utilization of grafting of dissolving pulp prepared from acrylamides and two by-products from *Phoenix dactylifera* L. (rachis and leaflet each alone) using (PPS) as initiator accomplished the goal of adsorption of MO dye from industrial water.

## References

- Agoudjil, B., A. Benchabane, A. Boudenne, L. Ibos, and M. Fois, 2011. Renewable materials to reduce building heat loss: Characterization of date palm wood. *Energy and buildings*, 43 (2-3): 491-497.
- Ahmed, I. A., A.W.K. Ahmed and R.K. Robinson, 1995. Chemical composition of date varieties as influenced by the stage of ripening. *Food chemistry*, 54 (3): 305-309.
- Al-Sulaiman, F.A., 2003. Date palm fibre reinforced composite as a new insulating material. *International Journal of Energy Research*, 27 (14): 1293-1297.
- Alvarez, C., B. Rojano, O. Almaza, O. J. Rojas, and P., Gañán, 2011. Self-bonding boards from plantain fiber bundles after enzymatic treatment: adhesion improvement of lignocellulosic products by enzymatic pre-treatment. *Journal of Polymers and the Environment*, 19 (1): 182-188.
- Bhattacharya, D., D. Ghoshal, D. Mondal, B.K. Paul, N. Bose, S. Das, and M., Basu, 2019. Visible light driven degradation of brilliant green dye using titanium based ternary metal oxide photocatalyst. *Results in Physics*, 12: 1850-1858.
- Boldizar, A., C. Klason, J. Kubat, P. Näslund, and P. Saha, 1987. Prehydrolyzed cellulose as reinforcing filler for thermoplastics. *International Journal of Polymeric Materials*, 11(4): 229-262.
- Brdar, M., Šćiban, M., Takači, A. and Došenović, T., 2012. Comparison of two and three parameters adsorption isotherm for Cr (VI) onto Kraft lignin. *Chemical Engineering Journal*, 183: 108-111.

- Brinchi, L., Cotana, F., Fortunati, E. and Kenny, J. M., 2013.** Production of nanocrystalline cellulose from lignocellulosic biomass: technology and applications. *Carbohydrate polymers*, 94 (1): 154-169.
- Ching, Y.C. and Ng, T.S., 2014.** Effect of preparation conditions on cellulose from oil palm empty fruit bunch fiber. *BioResources*, 9 (4): 6373-6385.
- Chirayil, C.J., J. Joy, L. Mathew, M. Mozetic, J. Koetz, and S. Thomas, 2014.** Isolation and characterization of cellulose nanofibrils from *Helicteres isora* plant. *Industrial Crops and Products*, 59: 27-34.
- Elseify, L.A., M. Midani, A.H. Hassanin, T. Hamouda, and R. Khiari, 2020.** Long textile fibres from the midrib of date palm: Physiochemical, morphological, and mechanical properties. *Industrial Crops and Products*, 151: 112466.
- EL-Torky, A.M., G.O. El-Sayed, and E.E. Abd-Elmonem, 2017.** Cu (II), Mn (II) and Zn (II) Adsorption with Modified Grafted Cellulose from Aqueous Solution. *Journal of Basic and Environmental science*, 4: 61-69.
- González-Bahamón, L.F., D.F. Hoyos, N. Benítez and C. Pulgarín, 2011.** New Fe-immobilized natural bentonite plate used as photo-Fenton catalyst for organic pollutant degradation. *Chemosphere*, 82 (8): 1185-1189.
- Gupta, V.K., D. Pathania, S. Sharma, S. Agarwal, and P. Singh, 2013.** Remediation and recovery of methyl orange from aqueous solution onto acrylic acid grafted *Ficus carica* fiber: isotherms, kinetics and thermodynamics. *Journal of Molecular Liquids*, 177: 325-334.
- Hassanzadeh-Tabrizi, S.A., M.M. Motlagh, and S. Salahshour, 2016.** Synthesis of ZnO/CuO nanocomposite immobilized on  $\gamma$ -Al<sub>2</sub>O<sub>3</sub> and application for removal of methyl orange. *Applied Surface Science*, 384: 237-243.
- He, Y., D.B. Jiang, J. Chen, and Y.X. Zhang, 2018.** Synthesis of MnO<sub>2</sub> nanosheets on montmorillonite for oxidative degradation and adsorption of methylene blue. *Journal of colloid and interface science*, 510: 207-220.
- Ho, Y.S. and A.E. Ofomaja, 2006.** Pseudo-second-order model for lead ion sorption from aqueous solutions onto palm kernel fiber. *Journal of hazardous materials*, 129(1-3): 137-142.
- Jawaid, M.H.P.S. and H.A. Khalil, 2011.** Cellulosic/synthetic fibre reinforced polymer hybrid composites: A review. *Carbohydrate polymers*, 86 (1): 1-18.
- Kaddami, H., A. Dufresne, B. Khelifi, A. Bendahou, M. Taourirte, M. Raihane, and N. Sami, 2006.** Short palm tree fibers–Thermoset matrices composites. *Composites Part A: Applied Science and Manufacturing*, 37 (9): 1413-1422.
- Khiari, R., S. Dridi-Dhaouadi, C. Aguir, and M.F. Mhenni, 2010.** Experimental evaluation of eco-friendly flocculants prepared from date palm rachis. *Journal of environmental sciences*, 22 (10): 1539-1543.
- Kumar, R., R.K. Sharma, and A.P. Singh, 2017.** Cellulose based grafted biosorbents–Journey from lignocellulose biomass to toxic metal ions sorption applications–A review. *Journal of Molecular Liquids*, 232: 62-93.
- Langmuir, I., 1918.** The adsorption of gases on plane surfaces of glass, mica and platinum. *Journal of the American Chemical society*, 40 (9): 1361-1403.
- Li, R., L. Liu, and F. Yang, 2014.** Removal of aqueous Hg (II) and Cr (VI) using phytic acid doped polyaniline/cellulose acetate composite membrane. *Journal of hazardous materials*, 280: 20-30.
- Li, Z., N. Potter, J. Rasmussen, J. Weng, and G. Lv, 2018.** Removal of rhodamine 6G with different types of clay minerals. *Chemosphere*, 202: 127-135.
- Lin, J., L. Fan, R. Miao, X. Le, S. Chen, and X. Zhou, 2015.** Enhancing catalytic performance of laccase via immobilization on chitosan/CeO<sub>2</sub> microspheres. *International journal of biological macromolecules*, 78: 1-8.

- Liu, K., L. Chen, L. Huang, and Y. Lai, 2016.** Evaluation of ethylenediamine-modified nanofibrillated cellulose/chitosan composites on adsorption of cationic and anionic dyes from aqueous solution. *Carbohydrate polymers*, 151: 1115-1119.
- Liu, Y., G. Zeng, L. Tang, Y. Cai, Y. Pang, Y. Zhang, and Y. He, 2015.** Highly effective adsorption of cationic and anionic dyes on magnetic Fe/Ni nanoparticles doped bimodal mesoporous carbon. *Journal of colloid and interface science*, 448: 451-459.
- Ma, C.C.M., H.T. Tseng and H.D. Wu, 1998.** Blocked diisocyanate polyester-toughened novolac-type phenolic resin: Synthesis, characterization, and properties of composites. *Journal of applied polymer science*, 69 (6): 1119-1127.
- Mahdavi, S., H. Kermanian and A. Varshoei, 2010.** Comparison of mechanical properties of date palm fiber-polyethylene composite. *BioResources*, 5 (4): 2391-2403.
- Mahmoodian, H., O. Moradi, B. Shariatzadeha, T.A. Salehf, I. Tyagi, A. Maity and V. K. Gupta, 2015.** Enhanced removal of methyl orange from aqueous solutions by poly HEMA–chitosan-MWCNT nano-composite. *Journal of Molecular Liquids*, 202: 189-198.
- Mostafa, H.Y., A.M.A. Nada, A.M.M. Elmasry and M.E. Mahdi, 2007.** Grafting copolymerisation of vinyl monomers onto cellulose Egyptian cotton linters. *Pigment & Resin Technology*, 36 (4): 241-248.
- O'sullivan, A.C., 1997.** Cellulose: the structure slowly unravels. *Cellulose*, 4(3), 173-207.
- Reyes-Luyanda, D., J. Flores-Cruz, P.J. Morales-Pérez, L.G. Encarnación-Gómez, F. Shi, P.M. Voyles and N. Cardona-Martínez, 2012.** Bifunctional materials for the catalytic conversion of cellulose into soluble renewable biorefinery feedstocks. *Topics in catalysis*, 55 (3-4): 148-161.
- Riahi, K., A.B. Mammou and B.B. Thayer, 2009.** Date-palm fibers media filters as a potential technology for tertiary domestic wastewater treatment. *Journal of Hazardous Materials*, 161(2-3): 608-613.
- Ristolainen, M., R. Alén, P. Malkavaara and J. Pere, 2002.** Reflectance FTIR microspectroscopy for studying effect of xylan removal on unbleached and bleached birch kraft pulps. *Holzforschung*, 56 (5): 513-521.
- Rosa, S.M., N. Rehman, M.I.G. de Miranda, S.M. Nachtigall and C.I. Bica, 2012.** Chlorine-free extraction of cellulose from rice husk and whisker isolation. *Carbohydrate Polymers*, 87 (2): 1131-1138.
- Rosas, J.M., J. Bedia, J. Rodríguez-Mirasol and T. Cordero, 2009.** HEMP-derived activated carbon fibers by chemical activation with phosphoric acid. *Fuel*, 88 (1): 19-26.
- Sbiai, A., A. Maazouz, E. Fleury, H. Souterneau and H. Kaddami, 2010.** Short date palm tree fibers/polyepoxy composites prepared using RTM process: effect of tempo mediated oxidation of the fibers. *BioResources*, 5 (2): 672-689.
- Segal, L., J.J. Creely, A.E. Martin, C.M. Conrad, 1959.** An empirical method for estimating the degree of crystallinity of native cellulose using the X-Ray diffractometer. *Text. Res. J.*, 29: 786–794.
- Sheltami, R.M., I. Abdullah, I. Ahmad, A. Dufresne and H. Kargarzadeh, 2012.** Extraction of cellulose nanocrystals from mengkuang leaves (*Pandanus tectorius*). *Carbohydrate Polymers*, 88 (2): 772-779.
- Simonin, J.P., 2016.** On the comparison of pseudo-first order and pseudo-second order rate laws in the modeling of adsorption kinetics. *Chemical Engineering Journal*, 300: 254-263.
- Somasundaram, S., K. Sekar, V.K. Gupta and S. Ganesan, 2013.** Synthesis and characterization of mesoporous activated carbon from rice husk for adsorption of glycine from alcohol-aqueous mixture. *Journal of Molecular Liquids*, 177: 416-425.

- Sun, H., X. Jin, N. Long and R. Zhang, 2017.** Improved biodegradation of synthetic azo dye by horseradish peroxidase cross-linked on nano-composite support. *International journal of biological macromolecules*, 95: 1049-1055.
- Yang, S., Y. Zhang, W. Yue, W. Wang, Y.Y. Wang, T.Q. Yuan, R.C. Sun, 2016.** Valorization of lignin and cellulose in acid-steam-exploded corn stover by a moderate alkaline ethanol post-treatment based on an integrated biorefinery concept. *Biotechnology for biofuels*, 9 (1): 238.
- Youssef, A.M., H. EL-Didamony, M. Sobhy and S.F. EL-Sharabasy, 2019.** Adsorption of Methylene Blue onto Chemically Prepared Activated Carbon from Date Palm Pits: Kinetics and Thermodynamics. *By-Products of Palm Trees and Their Applications*, 11: 275.
- Zhang, B., Y. Wu and L. Cha, 2020.** Removal of methyl orange dye using activated biochar derived from pomelo peel wastes: performance, isotherm, and kinetic studies. *Journal of Dispersion Science and Technology*, 41 (1): 125-136.
- Zhang, Y.H.P. and L.R. Lynd, 2006.** A functionally based model for hydrolysis of cellulose by fungal cellulase. *Biotechnology and bioengineering*, 94 (5): 888-898.
- Zhijiang, C., H. Chengwei, Y. Guang and K. Jaehwan, 2011.** Bacterial cellulose as a template for the formation of polymer/nanoparticle nanocomposite. *Journal of Nanotechnology in Engineering and Medicine*, 2(3) 031006 (6 pages).

## إستخدام اللب المستخلص من مخلفات النخيل في تنقية المياه الصناعية

مها صبحي السيد<sup>١</sup>، علاء الدين محمد التركي<sup>٢</sup>، عز الدين جاد الله حسين<sup>١</sup>  
<sup>١</sup>المعمل المركزي للأبحاث وتطوير نخيل البلح – مركز البحوث الزراعية.  
<sup>٢</sup>كلية العلوم – جامعة الزقازيق – قسم الكيمياء العضوية.

### الملخص العربي

اهتمت هذه الدراسة باستخلاص السليولوز من جريد النخيل والسعف بهدف تعظيم الإستفادة من مخلفات النخيل، وتم تحضير البوليمرات التطعيمية من السليولوز المستخلص من الجريد والسعف عن طريق استخدام الأكريلاميد في وجود البوتاسيوم بيرسلفات كعامل محفز (بادئ) لعملية البلمرة لكل علي حدة وتم تغير تركيز العامل المحفز (البادئ 0.6، 0.8) للتفاعل وذلك بغرض الحصول علي افضل نسبة تطعيم وافضل العينات كفاءة في إزالة الملوثات من الماء. وأظهرت نتائج التوصيف للميكروسكوب الالكتروني من وجود السليولوز النقي وبقياس طيف الاشعة تحت الحمراء تم التاكيد من وجود مجموعات مختلفة وظيفية تحتوي علي الكربونيل في عينات السليولوز المبلمرة. وتم دراسة امتزاز (صبغة methyl orange) باستخدام البوليمرات الناتجة من البلمرة التطعيمية لإزالة الصبغة من المياه الصناعية وكانت أفضل النتائج عند إستخدام البوتاسيوم بيرسلفات عند تركيز (0.8 للبادئ) في الوسط الحامضي لمدة ١٥ ساعة في حالة كلا من السليولوز المستخلص من الجريد والسعف الذي أظهر قدرة عالية على إزالة الملوثات من المياه كما أظهرت الدراسة الحركية أن التفاعل يتبع الرتبة الثانية. مما سبق يتضح أن السليولوز المعزول من مخلفات النخيل والمطعم بمادة الأكريلاميد قد حقق هدف امتزاز (صبغة methyl orange) من المياه الصناعية.

الكلمات الدالة: بلمرة تطعيمية للسليولوز، نخيل البلح، إزالة صبغة methyl orange